Pergamon

Int. J. Multiphase Flow Vol. 24, No. 1, pp. 145–162, 1998

Printed in Great Britain
PII: S0301-9322(97)00044-X
0301-9322/98 $19.00 + 0.00

STUDY ON THE DEFORMATION AND DEPARTURE OF A BUBBLE ATTACHED TO A WALL IN D.C./A.C. ELECTRIC FIELDS

Y. C. KWEON[1], M. H. KIM[2], H. J. CHO[3] and I. S. KANG[3]

[1]Mechanical Engineering Research Laboratory, KEPRI, 106-16 Munji-dong, Yusung-Gu, Taejon 305-380, South Korea
[2]Department of Mechanical Engineering, POSTECH, San 31, Hyoja-dong, Pohang 790-784, South Korea
[3]Department of Chemical Engineering, POSTECH, San 31, Hyoja-dong, Pohang 790-784, South Korea

(Received 13 March 1996; in revised form 27 May 1997)

Abstract—In order to investigate the effects of electric fields on the behavior of a bubble attached to a wall, basic experiments on the deformation and departure of a bubble are carried out under d.c./a.c. applied voltages. In the present study, three types of electrodes are used, to examine the bubble behavior by the nonuniformity of the electric field. For a d.c. electric field, as the applied voltage increases the bubble attached to a wall is more extended in the direction parallel to the imposed electric field, thus the aspect ratio and the contact angle also increase. The bubble departure volume in a nonuniform electric field decreases continuously, while that in a uniform electric field is nearly constant. The present results by the d.c. electric field show that the bubble behavior is significantly affected by the degree of the inhomogeneity of the electrode configuration. For an a.c. electric field, as a preliminary analysis, a general theory on an equivalent dynamic system is extended to derive the bubble oscillation frequency. The analysis predicts that the bubble departure occurs near a resonant frequency. It is observed that the departure process of a bubble in the a.c. electric field is associated with the bubble oscillation which is composed of three different regions. Near the critical voltage, the bubble departure volume drops suddenly. It is also found that the reduction of the bubble departure volume by the a.c. electric field is more effective than in the d.c. electric field case. © 1997 Elsevier Science Ltd

Key Words: electrohydrodynamics, electric field, bubble shape, bubble departure volume, bubble oscillation, oscillation frequency

1. INTRODUCTION

It has been widely recognized that an electric field enhances considerably nucleate boiling heat transfer. The effect of an electric field has received major attention because of its potential applicability to industrial situations. Thus, in order to understand electrohydrodynamic (EHD) phenomena of the nucleate boiling heat transfer enhancement, many experimental studies have been carried out (Lovenguth 1968; Jones 1978; Copper 1990; Ogata and Yabe 1991; Damianidis *et al.* 1992; Ohadi *et al.* 1992; Kweon *et al.* 1996). These studies have shown that the nonuniform electric field affects considerably the nucleate boiling process. Based on these experimental observations, it is suggested that the applied electric field may lead to the change in the bubble behavior, which is believed to be one of the main reasons for the nucleate boiling heat transfer enhancement. However, although EHD effects have long been observed in boiling systems, the basic mechanisms of the nucleate boiling heat transfer enhancement by the application of the electric field have not been clearly clarified yet. Therefore, fundamental studies on the bubble behavior in the nonuniform electric field are necessary for understanding the basic mechanisms of the EHD nucleate boiling process.

Due to the complexity of the EHD phenomena, most theoretical works have been performed for the bubble under a uniform d.c. electric field. The effects of the uniform d.c. electric field on the behaviors of a suspended bubble in a liquid medium had been studied by Garton and Krasuchi (1964), Melcher and Taylor (1969) and Miksis (1981). They showed that a bubble in a liquid medium was elongated in the direction parallel to the electric field. Cheng and Chaddock (1985,

1986) studied the shape and departure volume of a bubble attached to a wall in a uniform d.c. electric field. They expressed the dimensionless maximum bubble departure volumes in terms of the dimensionless electric field strength. Their results showed that the dimensionless electric field strength could be divided into two regions; a weak electric field region where the dimensionless volume is nearly constant and a strong electric field region where it decreased. Ogata and Yabe (1993) and Yabe *et al.* (1995) had carried out experiments and analyses on the behavior of bubbles attached to a wall in a semi-uniform d.c. electric field, in order to investigate the basic mechanism of the boiling heat transfer enhancement. They analyzed bubble behavior and the electric forces on a bubble and observed that bubbles were changed into longish ones. However, they did not report the results on the bubble shape and the departure volume in terms of the applied voltage. Cho *et al.* (1996) performed numerical analyses and experiments to investigate the effects of a uniform d.c. electric field on a bubble attached to a wall. The orthogonal curvilinear coordinate system was employed for the numerical studies. They obtained the steady bubble shape under the fixed contact radius condition. Their numerical and experimental results showed good agreement. In spite of the large number of studies of the bubble behavior, no theoretical or experimental works were published on the effect of an a.c. electric field on a bubble attached to the wall. As mentioned above, due to the intrinsic complexity of the EHD process, the majority of the previous researchers have used the uniform d.c. electric field to investigate the effects of an electric field on the bubble behavior under the static situation. The uniform electric field does not have significant effects for the nucleate boiling process. Therefore, there has been a need for basic experimental studies using the nonuniform electric field.

In the present study, the effects of an electric field on the behavior of a bubble attached to a wall are studied for both the uniform and nonuniform electric fields in d.c./a.c applied voltages. For this purpose, the bubble shape, departure volume, oscillation behavior and oscillation frequency are investigated. Thermal effects are supposed to play an important role in nucleate boiling heat transfer. The present work is, however, restricted to the bubble under isothermal conditions. Although the results addressed in this paper are not sufficient to describe the behavior of vapor bubbles in the boiling system, they may provide an initial perspective on the effects of the electric field on bubbles attached to a wall.

2. EXPERIMENTAL APPARATUS AND PROCEDURE

To investigate the effects of nonuniform d.c./a.c. electric fields on the deformation and departure of a single bubble attached to a wall, a bubble generator was designed and built. A schematic diagram of the bubble generator and three kinds of electrodes (Types 1, 2 and 3) are shown in figure 1. A bubble is generated by the injection of air through a stainless steel needle of length 50 mm, inner hole diameter 0.1 mm and outer diameter 0.7 mm. The experimental apparatus consists of plate or needle electrodes, d.c. or a.c. applied voltage power supply, high voltage probe and test chamber made of tempered glass to facilitate visual observations. The frequency f of the a.c. system is 60 Hz. A 30 kV d.c. or a.c. power supply is used as the high voltage source. The high voltage probe is used to accurately measure the d.c. or a.c. high voltage applied to the upper electrode, while the lower electrode is grounded. Types 1 and 2 consist of two parallel conducting electrodes (copper, 120 mm $\times$ 120 mm). Type 3 consists of an upper conducting electrode and a lower insulating electrode (Teflon, 120 mm $\times$ 120 mm). That is, the lower plate electrode of Types 1 and 2 indicates the conducting wall and that of Type 3 indicates the insulating wall. In the case of Types 2 and 3, the needle is vertically located at the center of the lower electrode.

If the ratio (L/W) of the gap (L) of two electrodes and the length (W) of the electrode is below about 0.375, the difference in electric field strength along the center line from the lower electrode to the upper electrode is within 0.7% (Takuma *et al.* 1985). In the present study, since L/W of Type 1 is below 0.38, the electric field between two parallel electrodes can be assumed to be uniform except in the vicinity of the edge of two parallel electrodes. The electric field in Types 2 and 3 is nonuniform under the influence of the needle located on the lower electrode. As the needle height increases, the nonuniformity of the electric field increases. In the case of Type 3, since the Teflon plate is the insulating boundary, the electric field converges only to the needle. This electric field

concentration makes the nonuniform electric field near the needle much stronger for Type 3 than Type 2. Three types of electrodes used in the present studies are selected to compare qualitatively the effects of the geometrically uniform or nonuniform electric field.

In the present experiment, in order to generate the nonuniform electric field, the plate and needle electrode are used. The important considerations on the use of the needle are the following two points. One is the repeated production of small bubbles similar to vapor bubbles departing at the heat transfer surface in boiling liquid. It is difficult to generate small bubbles on the heat transfer surface with regularity. The needle is one of the ways to produce a single bubble on the wall with regularity under carefully controlled conditions. The other is how the bubble is affected by the inhomogeneity of the electrode configuration. For the case of the plate and needle electrode, it is well known that this type of electrode configuration provides much more strongly nonuniform electric field than Type 2 (Duffin 1990). Thus, the vertical needle in a stationary liquid is considered. These are believed to provide the qualitative perspective on the effects of the electric field on bubbles attached to a wall.

Before each experiment, the electric field is applied between two electrodes. After the applied voltage is maintained under steady-state condition (within $\pm 0.5\%$ of the setting voltage), the air in a syringe is injected by rising the lifter until the bubble departs. A syringe with volume 100 μl is used. The bubble departure volume, which is achieved by careful consideration, is measured by the digital micrometer with an accuracy of $\pm 0.5\%$ of reading and is the mean value of 20 measurements taken at each d.c. or a.c. applied voltage, with a maximum $\pm 2\%$ deviation from mean values. Since the air flow injected into the working fluid is sufficiently slow, the pressure variations, inertia and viscous effects can be negligible. Experiments have been carried out changing electrode gaps (L = 16–36 mm), needle heights (H = 0–3 mm) and applied voltages (0–30 kV) for three types of electrodes.

The working fluid is cyclohexane, C_6H_{12}. The properties of cyclohexane are listed in table 1. The characteristic time of electric charge relaxation is about 780 ms for cyclohexane, which is expressed as the ratio of the permittivity and the electrical conductivity. This characteristic time of cyclohexane is longer compared with that of CFC alternatives, which is of the order of several 10 ms. This means that cyclohexane has relatively small interaction and influence of the electric field in comparison with CFC alternatives. In addition, since cyclohexane is a non-polar dielectric liquid with very poor conductivity, the electric current through cyclohexane can be negligible (the current measured in this study is of the order of microamps). As a result, it is assumed that there are no free charges in cyclohexane.

3. RESULTS

3.1. *Behavior of a bubble in a d.c. electric field*

3.1.1. *Effect of the nonuniformity of an electric field.* The effective electric body force $\mathbf{F}^{(e)}$ exerted on a dielectric liquid can be derived from the concept of electrostatic energy (Stratton 1941) as follows:

$$\mathbf{F}^{(e)} = \rho_c \mathbf{E} - \frac{1}{2} E^2 \nabla \epsilon + \frac{1}{2} \nabla \left(\rho E^2 \left(\frac{\partial \epsilon}{\partial \rho} \right)_T \right), \qquad [1]$$

where ρ_c, ϵ and $\mathbf{E}$ are the free charge density, the permittivity and the electric field strength. These terms present the electrophoretic, the dielectrophoretic and the electrostrictive forces. The first term is the Coulomb force acting on the free charges, which is assumed to be negligible in the present study, due to no free charge in the working fluid. The second term is the force produced by the spatial gradient of the permittivity. The third term is the force caused by the inhomogeneity of the electric field. The physical meanings of each term were introduced in detail by Yabe *et al.* (1995). In a nonuniform electric field, the net electrical force ($\mathbf{F}_d^{(e)}$) exerted on a bubble was expressed by Pohl (1958), based on the polarization concept. This force attracts a bubble towards the region of the weaker electric field and tends to pull the bubble off a wall more rapidly. As a result, bubbles

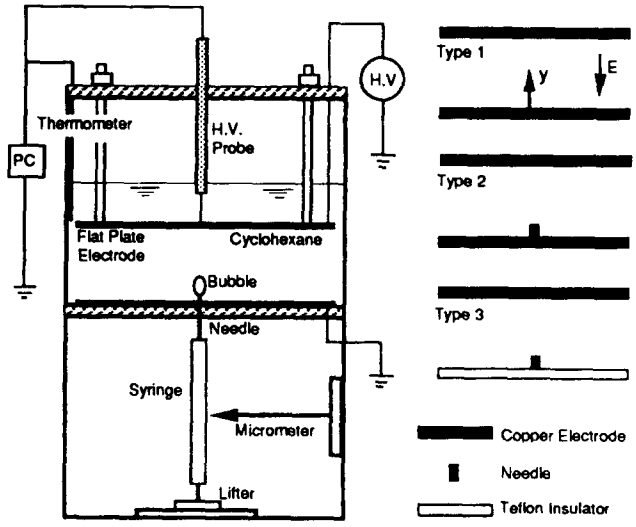

Figure 1. Schematic diagram of the experimental apparatus and the electrode systems.

of small size depart from the wall, as shown in many boiling studies using the nonuniform electric field.

Figure 2 shows normal electric field strengths for Types 1, 2 and 3 in a d.c. electric field, with electrode gap (L) of 16 mm and needle height (H) of 0 and 1 mm, where $\mathbf{E}_o$ and y are the uniform d.c. electric field strength ($\mathbf{E}_o = \phi/L$) and the coordinate axis normal to the lower electrode, respectively. Near the needle, the magnitude of $\mathbf{E}$ is the largest and its distribution is also inhomogeneous. Thus, a bubble on the needle may experience much larger electric effects than in the case of the flat plate. Figure 3 shows electric equipotential lines around a bubble attached to the wall ($H' = 0$) and needle ($H' = 1/3$ or $H' = 2/3$) in a d.c. electric field. Electric equipotential lines are obtained numerically using a boundary-fitted orthogonal coordinate system (Cho *et al.* 1996). Here, ϕ' and H' represent the relative electric potential and the relative needle height (needle height per electrode gap). In the case of $H' = 0$, the equipotential lines are curved in the vicinity of the bubble and are uniform far from the bubble, while in the case of $H' = 1/3$ or $H' = 2/3$, equipotential lines are remarkably distorted due to the needle that produces the nonuniform electric field. From these figures, we can see that the electric field becomes stronger near the bubble and also the degree of its nonuniformity increases as the needle height increases, compared with the case of the uniform electric field.

Figure 4 shows the variation of the electric normal force $\mathbf{S}_n$ exerted on a hemispherical bubble on the needle in a d.c. electric field. The normal force at the bubble surface can be given as follows:

$$\mathbf{S}_n = \mathbf{n}\cdot(\mathbf{T}_L - \mathbf{T}_G), \qquad [2]$$

where subscripts L and G represent liquid and gas phase, respectively, and $\mathbf{n}$ is the outgoing normal vector. The Maxwell stress tensor $\mathbf{T}$ presented in the above expression is defined as

$$\mathbf{T} = \epsilon\left[\mathbf{EE} - \frac{1}{2}E^2\mathbf{I}\right]. \qquad [3]$$

Table 1. Physical properties of C_6H_{12} at 20°C

ρ (density)	949 kg/m^3
μ (viscosity)	0.92×10^{-3} Ns/m^2
ϵ (permittivity)	1.948×10^{-11} F/m
γ (surface tension)	2.45×10^{-2} N/s
σ (conductivity)	2.5×10^{-11} S/m

Taken from Kagaku Binran, 2nd edn. Maruzen, in Japanese.

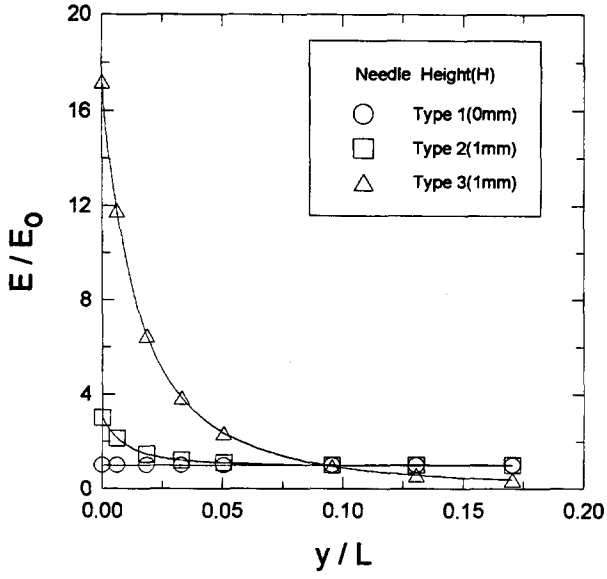

Figure 2. Normal electric field strengths for Types 1, 2 and 3 with electrode gap (L) of 16 mm.

Since the electric normal force is in the opposite direction to **n**, the normal force suppresses the bubble surface. When $H' = 1/3$ or $H' = 2/3$, the normal force exerted on the bubble is larger compared with the case of $H' = 0$. The electric force increases with increase of the needle height. The magnitude of the electric force is stronger at the lower side ($\theta > 60°$) than the pole of the bubble ($\theta = 0°$). From these figures, it is expected that the degree of the bubble deformation can be significantly affected by the electrode configuration.

3.1.2. *Bubble shape*. Figure 5 shows the evolution of bubble growth for the case of no and nonuniform electric fields, at a circular hole in isothermal conditions. Without an electric field, a bubble grows spherically. In the presence of the nonuniform electric field, however, it is found that the initial stage of bubble growth is not spherical shaped and the bubble is extended in a direction parallel to the applied electric field. This fact is crucial for the understanding of the bubble behavior in the EHD boiling process. As mentioned before, the previous theoretical works have been analyzed for an initially hemispherical or spherical bubble in the presence of an electric field. Thus, the analyses are not rigorous in the sense that they are based on the spheroidal method for a study of the bubble behavior in a real boiling system.

The shapes of the bubble attached to the electrode in the uniform and nonuniform electric fields are presented in figures 6(a)–(c). Figure 6(a) is the deformed shape of a bubble attached to the conducting bottom electrode without the needle. By increasing the applied voltage, the bubble becomes extended in a direction parallel to the electric field. Figures 6(b) and (c) are the deformed shape of a bubble attached to the conducting and insulating bottom electrodes with the needle. From these figures, we can see that the nonuniform electric field affects the bubble shape considerably. In the case of Type 3, as the applied voltage increases, the elongation of the bubble attached to a wall becomes steeper and then the bubble has a shape with slender waist at the lower side of the bubble. This shape is due to the inhomogenous distribution of the normal force acted on the bubble surface (see figure 4). Figure 7 shows the variations of the relative aspect ratio and the contact angle in the electric field, where AR_0 represents the aspect ratio of a bubble in the case of no electric field. The aspect ratio and the contact angle increase almost linearly with increasing applied voltage. Especially, the tendency of the relative aspect ratio and the contact angle increase is prominent for the case of Type 3 with the insulating bottom electrode, due to the electric field concentration near the needle. From these results, it may be concluded that the bubble deformation is largely affected by the inhomogeneity of the electrode configuration.

3.1.3. *Bubble departure volume*. The bubble departure volume is also affected by the strength and nonuniformity of the electric field. Figure 8 shows the bubble departure volume for the case of Type 1. The present experimental data are compared with the analytical result of Cheng

and Chaddock (1986), where V_0 is the bubble departure volume in the absence of the electric field. The experiment value, electrode gap 16 mm and applied voltage 20 kV, corresponds to about 0.916 of the dimensionless electric field strength $\epsilon_0 E^2/\sqrt{\gamma\rho g}$ introduced by Cheng and Chaddock. The bubble departure volume is nearly constant over the entire applied voltage examined, even though the strength of the uniform electric field increases. As shown in figure 10, this is because the electric force exerted on the bubble under the uniform electric field is weak. Experimental results are in good agreement with the analytical result. Figure 9 shows the bubble departure volume for the

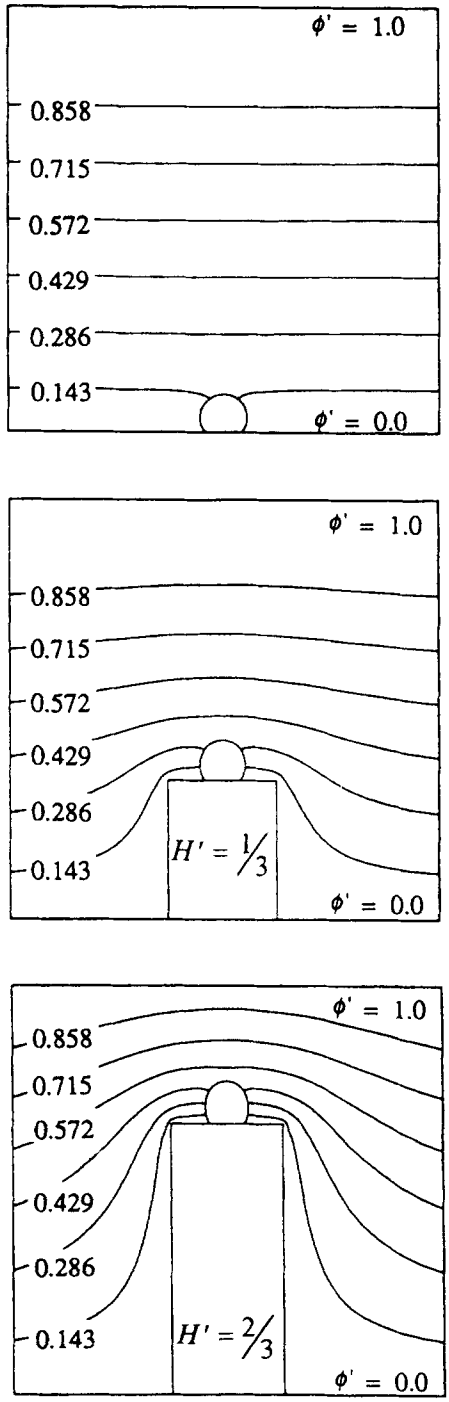

Figure 3. Electric equipotential lines around a bubble attached to a wall ($H' = 0$) or needle ($H' = 1/3$ or $H' = 2/3$).

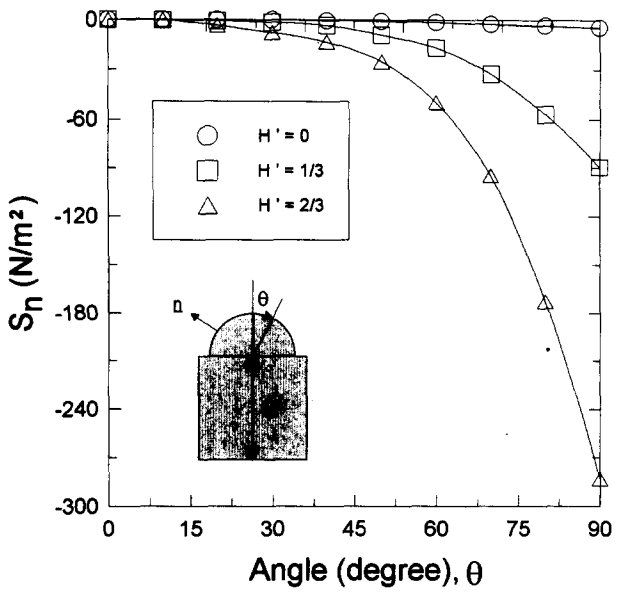

Figure 4. Variation of the electrical normal force exerted on a bubble attached to a wall ($H' = 0$) or needle ($H' = 1/3$ or $H' = 2/3$).

case of Types 2 and 3. The reduction of the bubble departure volume is very remarkable, as the needle height increases and the electrode gap decreases. In contrast to the case of the uniform electric field, the bubble departure volume in the nonuniform electric field decreases continuously as the applied voltage increases. The bubble departure volume for Type 3 is the smallest. Even though the applied voltage is very low, the reduction rate of the bubble departure volume is very large due to the strongly nonuniform electric field. For example, at about 2 kV d.c., the bubble departure volume in Type 3 is equivalent to about 20% of that affected by a uniform electric field. This verifies the fact that the vapor bubbles in boiling liquid subjected to a strongly nonuniform electric field may depart with a considerably smaller size than in the case of no electric field condition, as shown in EHD nucleate boiling studies (Choi 1962; Jones 1978; Ogata and Yabe 1993; Kweon *et al.* 1996).

3.1.4. *Electric-force on a bubble.* The electric field affects the dynamic behavior of bubbles. When an electric field is applied, the electric force ($\mathbf{F}_{e,s}$) exerted on the bubble can be obtained from the static force balance of a bubble attached to a wall, including the buoyancy, surface tension and electric force. The increase of the contact angle due to the electric field means that of the effective surface tension force ($\gamma \sin \theta_{c,s}$) between a bubble and a wall, where the subscript s means the static condition. The force balance of the bubble attached to the wall can be represented as

$$\pi D_h \gamma \sin \theta_{c,s} = \frac{\pi}{6} \Delta\rho g D_{b,s}^3 + \mathbf{F}_{e,s}, \qquad [4]$$

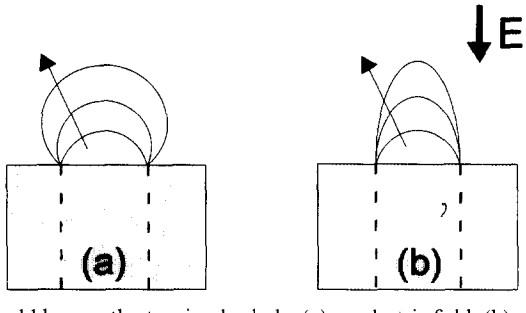

Figure 5. Evolution of bubble growth at a circular hole: (a) no electric field; (b) nonuniform electric field.

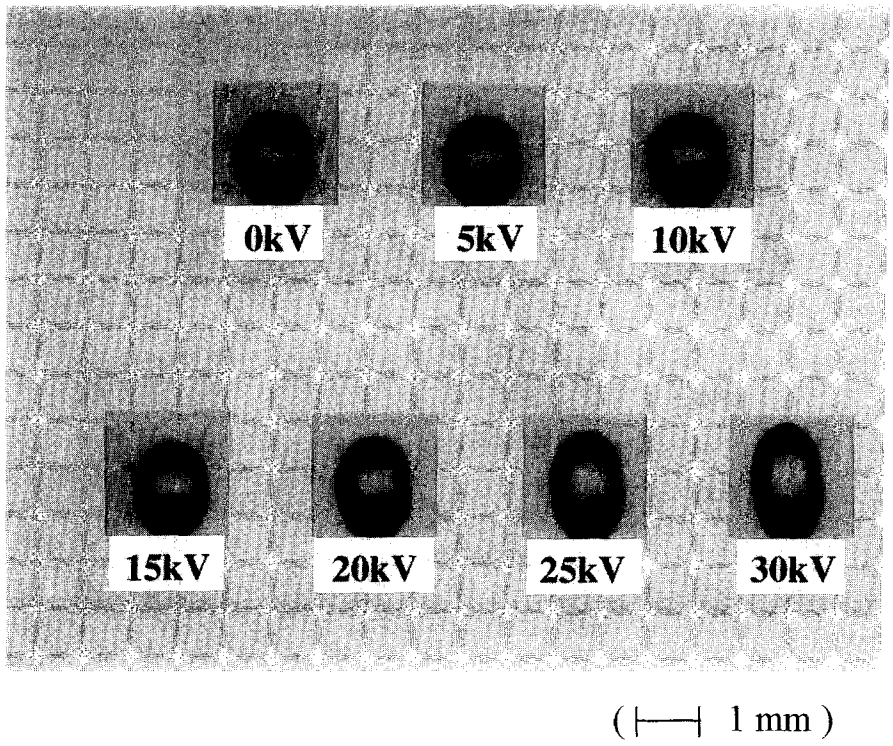
0kV
5kV
10kV
15kV
20kV
25kV
30kV
(⊢⊣ 1 mm)

Fig. 6(a).

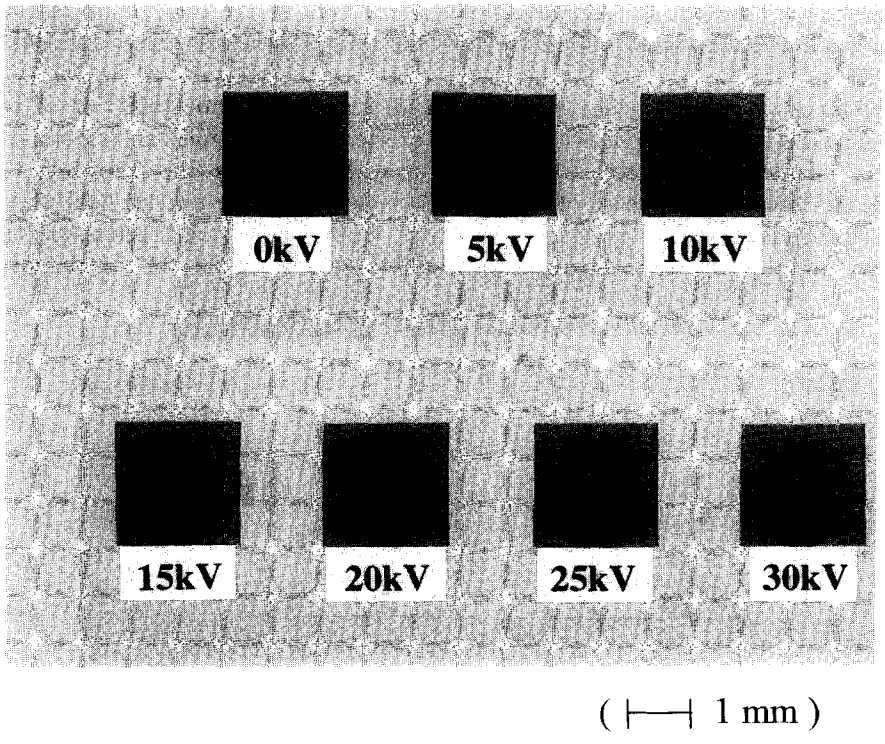
0kV
5kV
10kV
15kV
20kV
25kV
30kV
(⊢⊣ 1 mm)

Fig. 6(b).

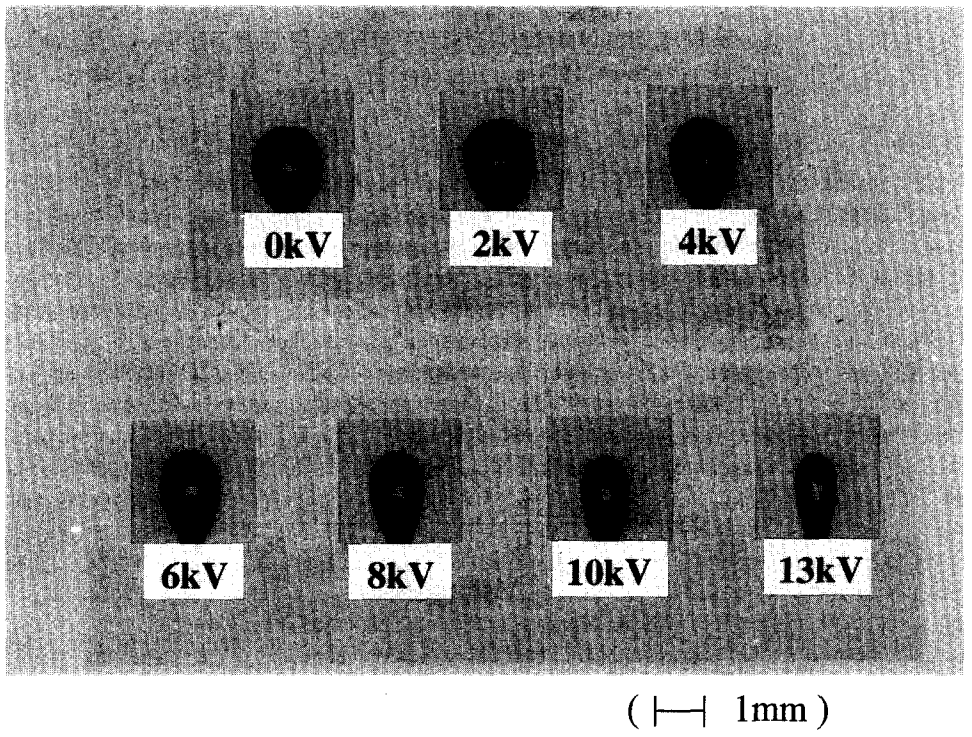

Fig. 6(c).

Figure 6. Experimental visualizations of the shape of a bubble attached to (a) a wall (Type 1); (b) the needle (Type 2); (c) the needle (Type 3).

where D_h and $D_{b,s}$ are the inner hole diameter and the static bubble equivalent diameter and $\theta_{c,s}$ is the static contact angle. Figure 10 shows the ratios of the static electric force and the surface tension force for the case of Types 1, 2 and 3. The static electric force exerted on a bubble is calculated from the force balance. The magnitude of the electric force increases as the applied voltage increases. The figure shows that the electric force exerted on the bubble increases as the electrode configuration is inhomogeneous. Even if the applied voltage is the same, the electric force is much higher in the case of Type 3 due to the concentration effect of the electric field near the needle. From these results, we can see that the strongly nonuniform electrical field has a significant influence on the dynamic behavior of bubbles. In addition, the electric force may affect the bubble departure process. It is observed from our visualizations that the bubble departure velocity increases by increasing the applied voltage or the needle height. It is also noted that the effects of the electric field on the bubble behavior in a nonuniform electric field are different from those for the case of applying uniform electric field.

3.2. *Behavior of a bubble in an a.c. electric field*

So far, we have considered the d.c. electric field. As mentioned in the Introduction, in contrast to the case of d.c. electric field, no efforts to investigate the effects of an a.c. electric field on bubble behavior have been reported. Thus, it is necessary to investigate the effects of the a.c. electric field. In this case, the important question is will the bubble behavior keep up with the changes in the electric field (Purcell 1965)? If the change in the a.c. electric field is over a very long period, it is supposed that the electric field becomes the same as in the d.c. electric field. In the present study, the change in the a.c. electric field is over a very short period compared with the characteristic time of the electric charge relaxation. Therefore, the electric field exerted on the bubble in the a.c. electric field may be different from that for the d.c. case. Moreover, due to the oscillation motion of a bubble, the a.c. electric field lines around a bubble may be changed. Thus, for a precise understanding of the a.c. electric field, the distribution of the electric field around an oscillating bubble should be analyzed.

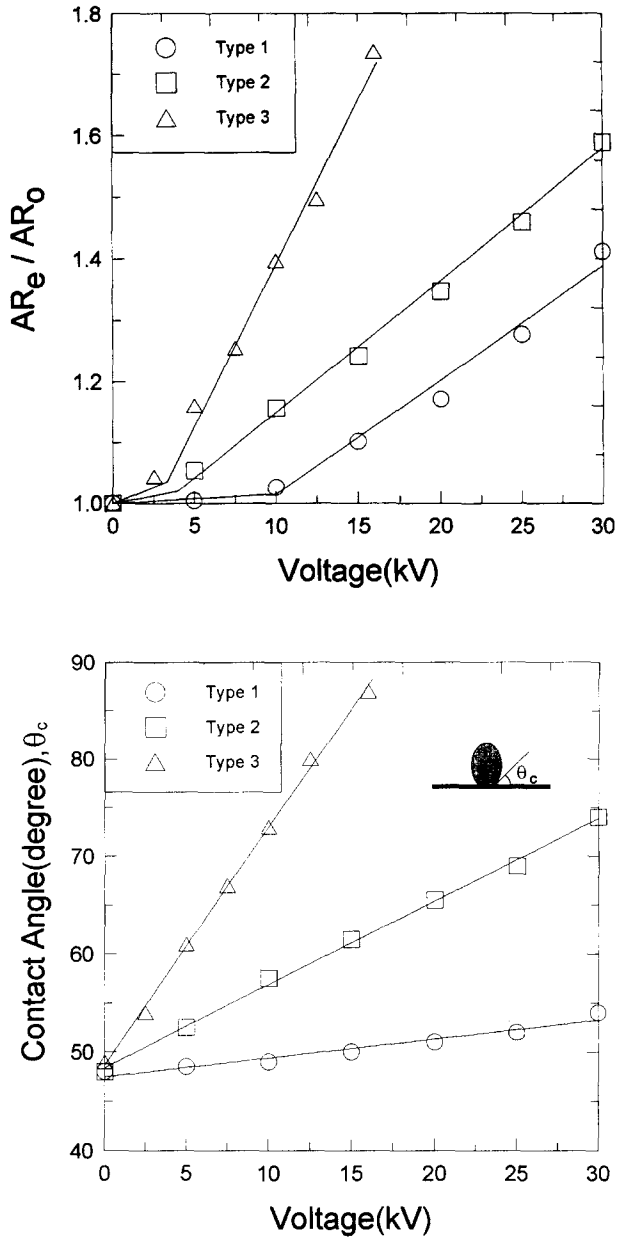

Figure 7. Variation of the relative aspect ratio and the contact angle (Types 1, 2 and 3).

The fundamental importance in bubble dynamics under the a.c. electric field is the oscillation behavior of a bubble, which is believed to be one of the field phenomena. Thus, the basic studies on the effects of the a.c. electric field are necessary for understanding the oscillation behavior of a bubble attached to a wall. As a preliminary analysis, the effect of the a.c. electric field on the bubble oscillation frequency has been studied by using a simple oscillation model in this paper.

3.2.1. *Bubble departure volume*. The bubble departure volume for the case of a nonuniform a.c. electric field (Types 2 and 3) is shown in figure 11. The bubble departure volume decreases as the applied voltage increases. The reduction effect of the bubble departure volume is most considerable in the case of Type 3. At a particular voltage, the bubble departure volume decreases suddenly. This voltage is named the critical voltage in this study. The critical voltage occurs at lower applied voltage as the electrode gap decreases and the needle height increases, that is, the critical voltage may strongly depend on the electrode configuration. From the present experimental results, it is found that there exist three regions for the bubble departure volume.

Regions I and II are the regions where the bubble departure volume decreases continuously, while Region II is the region where the bubble departure volume drops suddenly. At the relative bubble volume (V/V_o) of about 0.82, the bubble starts to oscillate with a small amplitude. At the relative bubble volume of 0.75–0.77, the bubble oscillates violently and then the relative bubble volume drops to about 0.26–0.28. This tendency is not observed in the present d.c. electric field experiment. This sudden reduction of the bubble departure volume is due to the resonance effect that oscillates extremely the bubble attached to the wall near the critical voltage. Comparing figure 9 with figure 11, we can see that the decrease in bubble departure volume by the a.c. electric field is much more efficient than in the d.c. electric field case as the applied voltage increases, within the region beyond the critical voltage.

3.2.2. *Bubble shape and oscillation.*The shape and oscillation of a bubble in the a.c. electric field are shown in figures 12(a)–(c). Figure 12(a) shows the oscillating bubble near the critical voltage (a.c. 21.5 kV) for Type 1, taken at the lower shutter speed (1/15 s) at an interval of 0.286 s. It is observed from this figure that the oscillating amplitude of the bubble increases linearly with time and the maximum oscillating amplitude (X) is almost equal to about 0.4 times the equivalent bubble departure diameter (D_b), that is $X/D_b \approx 0.4$. Figure 12(b) shows the deforming bubbles taken at the high shutter speed (1/500 s). This photograph is a snapshot of the bubble oscillating in the a.c. electric field. Figure 12(c) shows the oscillating bubble for Type 2, at an interval of 3 kV. The oscillation of the bubble is observed from about 12 kV a.c., which is shown by the dim shadow over the top of the bubble. At about 21 kV a.c., the bubble oscillates violently and then departs suddenly from the wall, as a result, the bubble departure occurs at a much smaller volume. From these visualization results, we can suppose that the oscillation phenomenon of a bubble due to the a.c. electric field promotes EHD convection effects such as the turbulence mixing and the disturbance of a fluid around a bubble attached to a wall in a stationary liquid.

3.2.3. *Analysis of an oscillating bubble.* Considering figure 12, in order to describe the oscillating behavior of a bubble attached to a wall, we consider the oscillating bubble as the equivalent dynamic system. As a preliminary analysis, the general theory on an equivalent dynamic system is extended to derive the oscillation frequency of a bubble attached to a wall in an a.c. electric field. With an electric force $\mathbf{F}(t)$ applied to the bubble, the bubble oscillates with a displacement $x(t)$, considered positive in the upward direction. The density and viscosity of the liquid are ρ and μ, and the surface tension γ is assumed to be uniform in the electric field. Letting

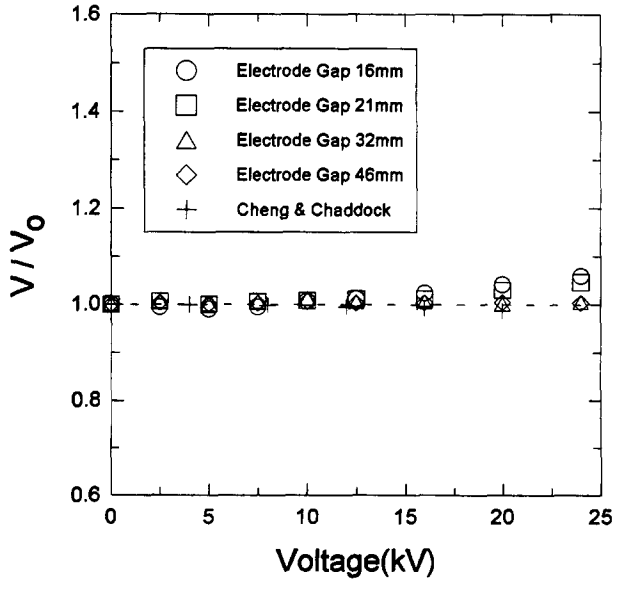

Figure 8. Relative bubble departure volume in the uniform d.c. electric field (Type 1).

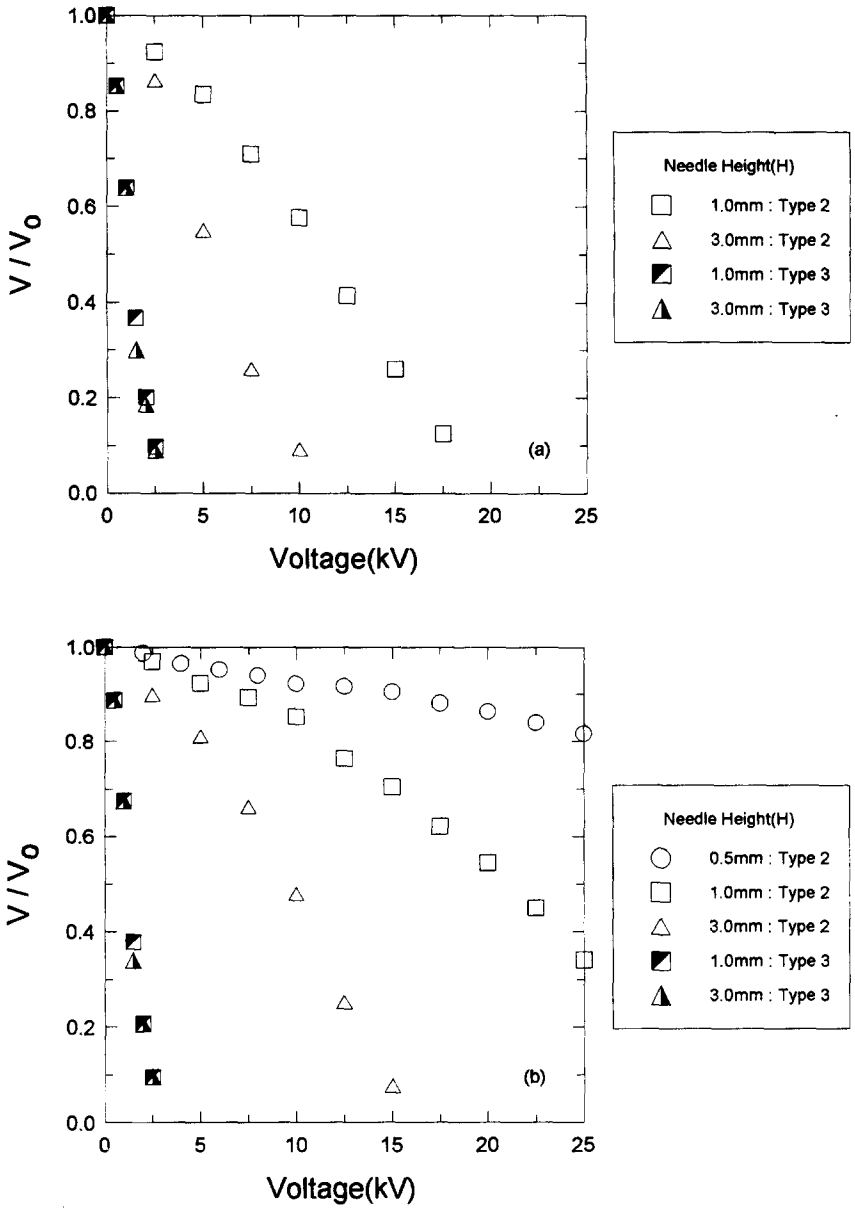

Figure 9. Relative bubble departure volume in the nonuniform d.c. electric field (Types 2 and 3): (a) electrode gap (L) 16 mm; (b) electrode gap (L) 32 mm.

the electric force be $\mathbf{F}(t) = \mathbf{F}_e \cos(2\pi f)t$, the balance of forces on a bubble due to elongation of the stiffness and the viscosity can be written in the form

$$M_b\ddot{x} + C_b\dot{x} + K_b x = \mathbf{F}_e \cos(2\pi f)t, \qquad [5]$$

where $M_b = C_1\pi\Delta\rho D_b^3/6$ and $C_b = \mu D_b$. The variable M_b is the equivalent bubble mass and is determined by the bubble departure diameter D_b. The constant C_1 is used to consider the bubble deformation. It means the effective mass fraction of the bubble which takes part in the bubble oscillation. For the solid particle, the value of this constant is one. The variable C_b is the equivalent viscous coefficient due to the fluid viscosity. Another variable K_b is the equivalent stiffness coefficient, which is defined as the ratio of the surface tension force acting on the bubble and the amplitude of the oscillating bubble, that is $K_b = 2\pi D_h\gamma(\sin\theta_{c,m} - \sin\theta_{c,o})/X_m$. Here D_h and X_m are the hole diameter and the maximum oscillating displacement of a bubble, respectively. $\theta_{c,o}$ and $\theta_{c,m}$ are the contact angle measured without and with applied voltage, and the subscript m indicates

maximum. It is generally assumed that the displacement of the mass center of the oscillating bubble is half the maximum oscillating displacement. The maximum oscillating displacement is about 0.4 times the equivalent departure diameter, based on the present experiment.

The LHS of [5] consists of the inertia, viscous and electric forces and the RHS is the electric force induced by the application of the a.c. electric field. The present analysis is based on the one-dimensional approximation. Thus, although this approximation model does not represent the detailed oscillation behavior of the bubble, it is helpful for understanding the potential of the oscillation behavior of a bubble attached to the wall. This may display one of the essential features of the oscillating bubble. When the oscillation frequency of a bubble attached to the wall coincides with that of the a.c. electric field, resonance occurs, and then its magnitude increases considerably. Rearranging [5] and solving the oscillation frequency of the bubble attached to the wall, one obtains,

$$f_n = \frac{1}{2\pi}\left(\frac{30D_h\gamma(\sin\theta_{c,m} - \sin\theta_{c,o})}{C_1\Delta\rho D_b^4}\right)^{1/2}. \quad [6]$$

For the resonance condition, C_1 is about 0.037. In order to calculate the oscillation frequency of the bubble attached to the wall, $\theta_{c,o}$ and $\theta_{c,m}$ are used as 48° and 75°, respectively. This equation shows that the oscillation frequency of a bubble on the wall is a function of the contact angle as well as the bubble departure diameter.

Figure 13 shows the oscillation frequency ($f_{n,e}/f_{n,o}$) of a bubble attached to a wall in the a.c. electric field as a function of the departure diameter, where $f_{n,o}$ is the bubble oscillation frequency in the absence of the electric field. The equivalent bubble diameter is measured at the moment that the bubble departs at the electrode. The subscript e indicates an electric field. The figure shows that the smaller the bubble departure diameter, the larger its oscillation frequency. As presented in figure 11, as the a.c. applied voltage increases, the bubble departure diameter decreases. Thus, the bubble oscillation becomes higher than in the no electric field case especially, which is particularly noticeable in the case of a bubble of smaller size. Figure 14 shows the ratios of the bubble oscillation frequency and the applied a.c. frequency for the case of Types 2 and 3 (H = 1, 3 mm and L = 16, 32 mm). The bubble oscillation frequency increases with increasing applied voltage. At the critical voltage, there is the transient rising region of the bubble oscillation frequency and then the bubble oscillation frequency increases two-fold. This fact may explain why the dynamic motion of a bubble becomes very unstable near the critical voltage.

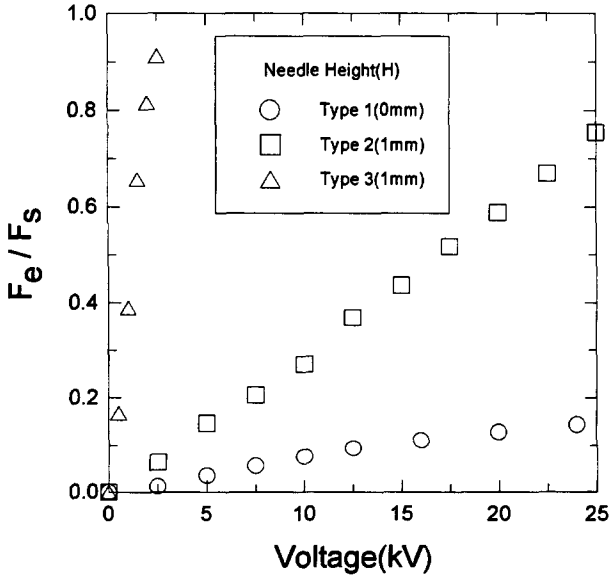

Figure 10. Ratios of the static electric forces and the surface tension force (Types 1, 2 and 3) (electrode gap L = 32 mm).

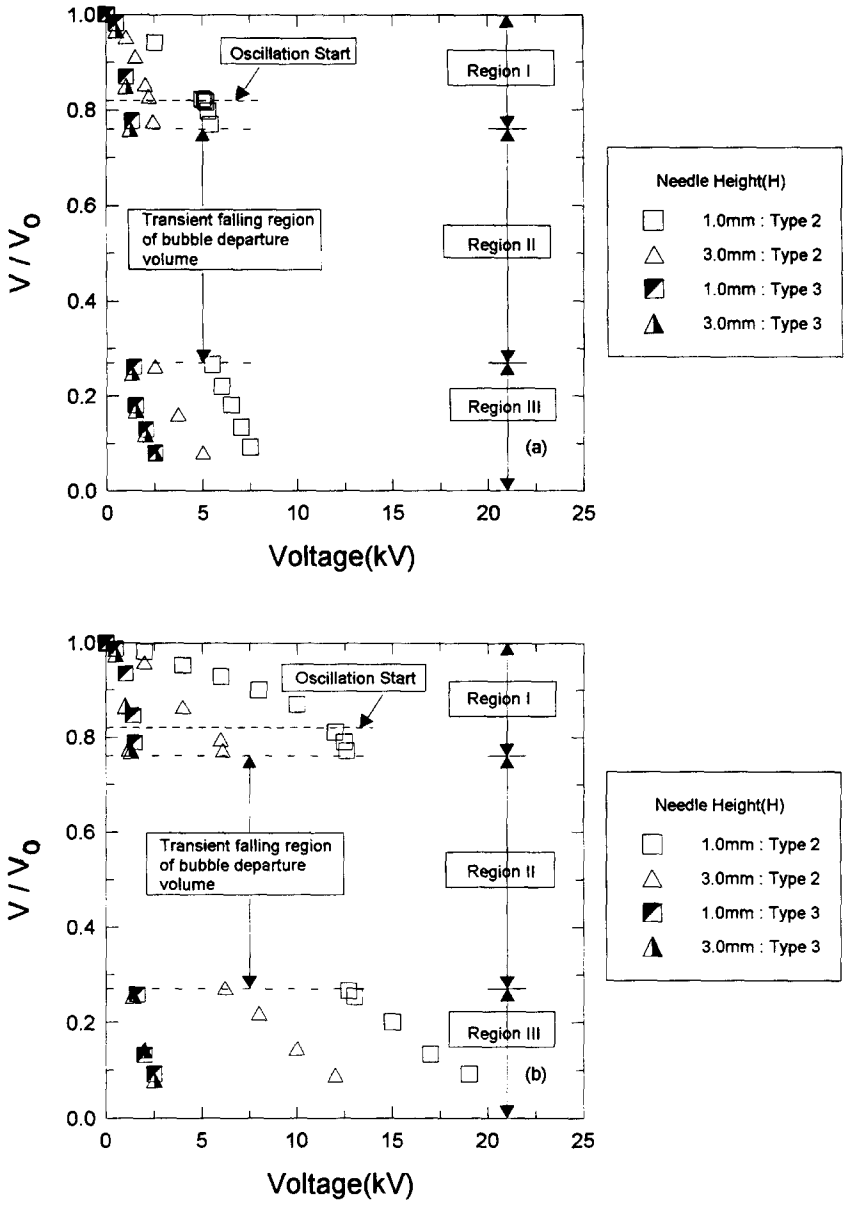

Figure 11. Relative bubble departure volume in the nonuniform a.c. electric field (Types 2 and 3): (a) electrode gap (L) 16 mm; (b) electrode gap (L) 32 mm.

These results may be believed to provide an initial perspective on the bubble oscillation as a starting point for the more detailed investigations of the bubble behavior in the a.c. electric field. From present studies. the departure mechanism of an oscillating bubble may be explained as follows.

Region 1. The bubble departure process depends on the buoyancy force and the electric force, like in the d.c. case. Since the applied voltage is below the critical voltage, the electric force $\mathbf{F}_e$ is smaller than the critical electric force $\mathbf{F}_{e,c}$ and the oscillating magnitude X of a bubble is below $0.4D_b$ ($\mathbf{F}_e < \mathbf{F}_{e,c}$, $X/D_b < 0.4$). If the amplitude of the electric force is small the bubble overcomes the resonance and reaches over the resonance region. In the early state of the bubble generation, the slight bubble oscillation is observed. As the bubble grows, however, the bubble oscillation disappears. That is, the departure of the bubble does not happen because the oscillation effect that promotes the dynamic behavior of the bubble is weak.

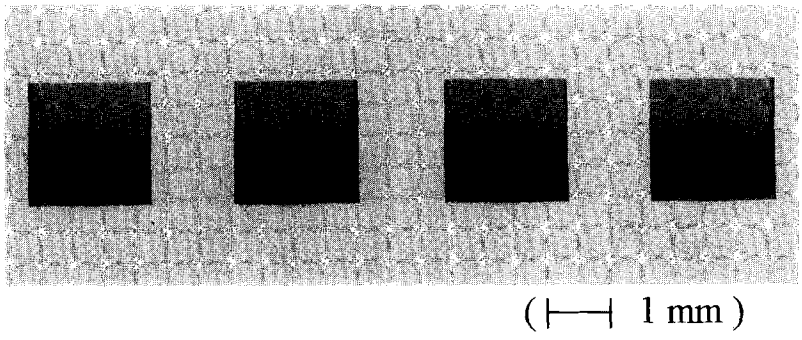

Fig. 12(a).

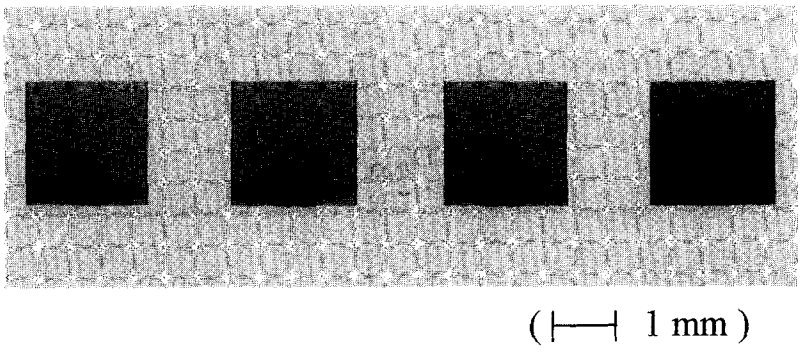

Fig. 12(b).

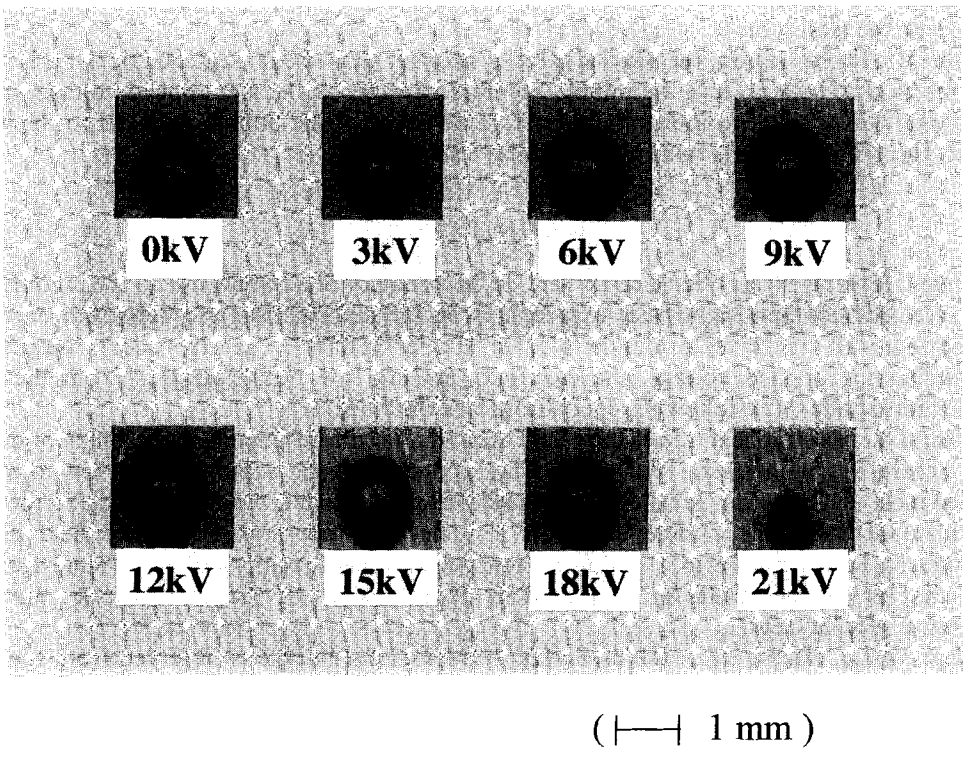

Fig. 12(c).

Figure 12. Experimental visualizations of the shape of (a) a bubble attached to a wall (Type 1); (b) a deforming bubble attached to a wall (Type 1); (c) a bubble attached to the needle (Type 2).

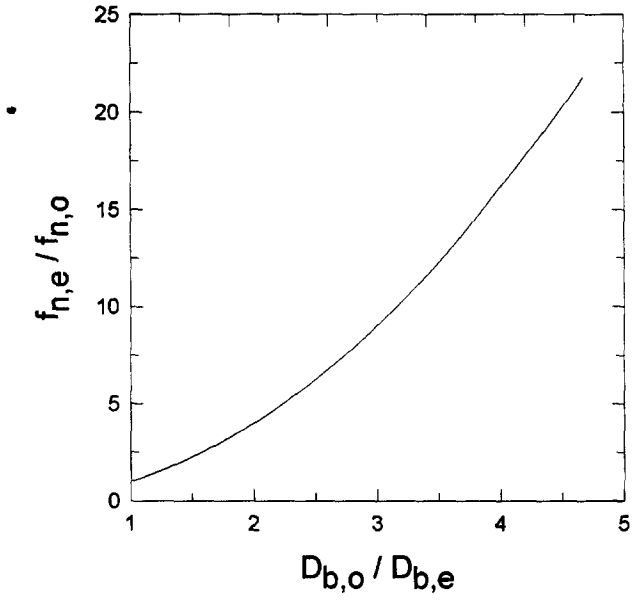

Figure 13. Relative oscillation frequencies of a bubble attached to a wall in an a.c. electric field.

Region II. As shown in figures 11 and 12, the bubble departs suddenly near the critical voltage. The electric force and the maximum oscillating displacement come to the critical electric force $\mathbf{F}_{e,c}$ and $0.4D_b$ ($\mathbf{F}_e \approx \mathbf{F}_{e,c}$, $X/D_b \approx 0.4$). If the amplitude of the electric force is larger, the bubble cannot overcome the resonance. At the resonance where the amplitude of the electric force reaches a critical value, bubble departure occurs. Thus, a sudden reduction of the bubble departure volume is observed in this region. This resonant frequency is related to the disturbance around a bubble attached to the wall.

Region III. In this region, the electric force is stronger than the critical electric force ($\mathbf{F}_e > \mathbf{F}_{e,c}$). Thus, the electric field around the bubble becomes stronger as the a.c. applied voltage increases. This strong electric field promotes the departure behavior of the bubble attached to the wall. As a result, the bubble departs with much smaller volume.

4. CONCLUSIONS

To investigate the effects of an electric field on the behavior of a bubble due to the inhomogeneity of the electrode configuration, basic experiments on the deformation and departure of a bubble attached to a wall are carried out under d.c./a.c. applied voltages. The experiments are performed by changing the applied voltage, the electrode gap and the needle height. From the present experimental studies, the following conclusions are obtained.

(1) For a d.c. electric field, the electric field around a needle becomes more strongly nonuniform as the needle height increases. With increasing applied voltage, a bubble attached to a wall is extended more in a direction parallel to the electric field. As a result, the aspect ratio and the contact angle also increase. The bubble departure volume in a nonuniform electric field decreases continuously, however, that in a uniform electric field is nearly constant. It is found from these results that the bubble behavior is dependent on the effects of the geometrically uniform or nonuniform electric field.

(2) For an a.c. electric field, the oscillating behavior of a bubble is observed from the present studies. As a preliminary analysis, general theory on an equivalent dynamic system is extended to derive the oscillation frequency of a bubble attached to a wall. The analysis predicts that the bubble departure occurs near the resonant frequency and then the bubble oscillation frequency increases two-fold. It is also found that the bubble departure process is composed of three regions. At the critical voltage, the bubble departure volume drops suddenly. Compared with the results of the d.c. case, the reduction of the bubble departure volume is more remarkable in an a.c. electric field, above a critical voltage.

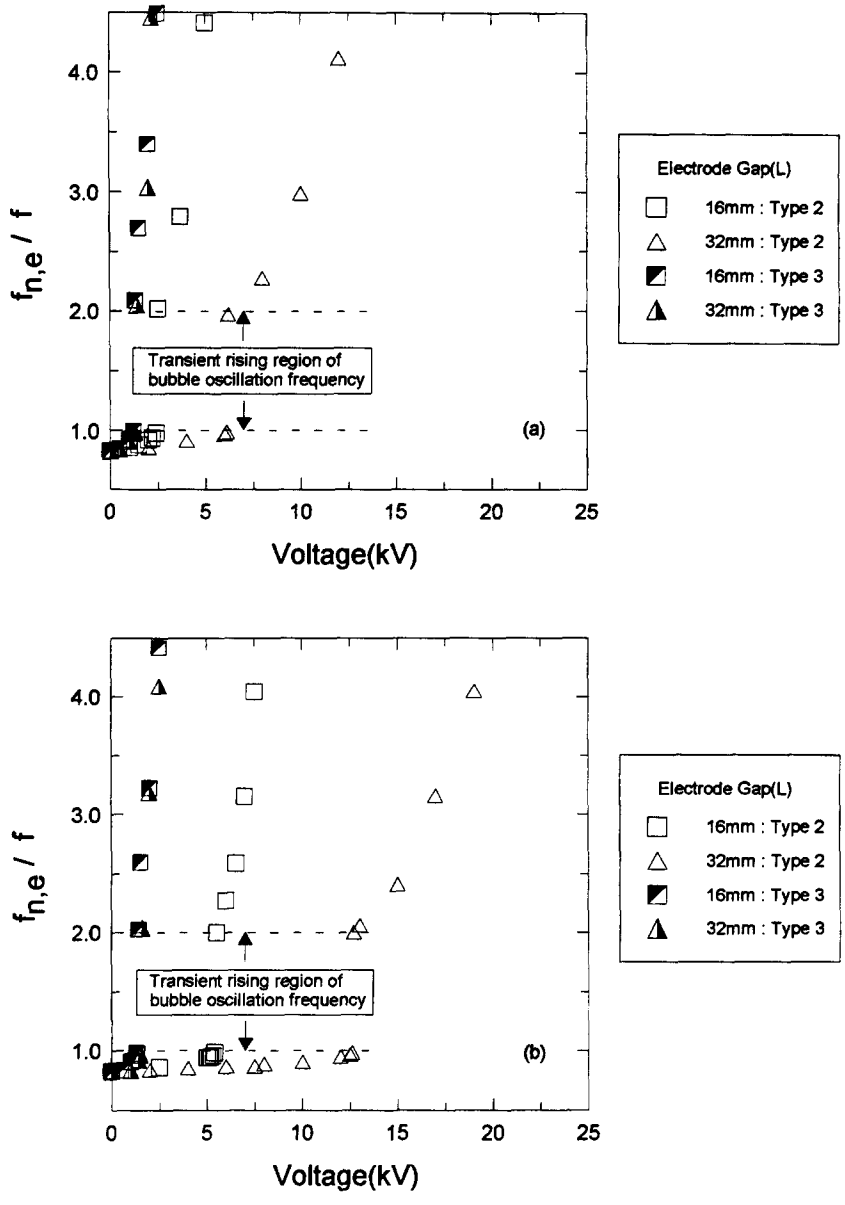

Figure 14. Comparison between the bubble oscillation frequency and applied a.c. frequency (Types 2 and 3): (a) needle height (H) 3 mm; (b) needle height (H) 1 mm.

Acknowledgements—The authors wish to thank the referees for their valuable suggestions and comments. This work was supported by a grant from the Korea Institute of Machinery and Metals and the Advanced Fluids Engineering Research Center at the Pohang University of Science and Technology.

REFERENCES

Cheng, K. J. and Chaddock, J. B. (1985) Effect of an electric field on bubble growth rate. *Int. Comm. Heat. Fluid Flow* **12,** 259–268.

Cheng, K. J. and Chaddock, J. B. (1986) Maximum size of bubbles during nucleate boiling in an electric field. *Int. J. Heat Fluid Flow* 7(4), 278–282.

Cho, H. J., Kang, I. S., Kwoen, Y. C. and Kim, M. H. (1996) Study on the behavior of a bubble attached to the wall in a uniform electric field. *Int. J. Multiphase Flow* **22,** 909–922.

Choi, H. Y. (1962) Electrohydrodynamic boiling heat transfer. Ph.D. Thesis, Mechanical Engineering Dept., MIT.

Copper, P. (1990) EHD enhancement of nucleate boiling. *J. Heat Transfer* **112,** 458–464.

Damianidis, C., Karayiannis, T. G., Al-Dadah, P. K., James, R. W., Collins, M. W. and Allen, P. H. G. (1992) EHD boiling enhancement in shell-and-tube evaporators and its application in refrigeration plants. *ASHRAE Trans. Symp.* **BA-92-5-5,** pp. 462–472.

Duffin, W. J. (1990) *Electricity and Magnetism*. McGraw-Hill, London.

Garton, C. G. and Krasuchi, Z. (1964) Bubbles in insulating liquids: stability in an electric field. *Proc. Roy. Soc. London* **A280,** 211–226.

Jones, T. B. (1978) Electrohydrodynamically enhanced heat transfer in liquids—A review. *Adv. Heat Transfer* **14,** 107–148.

Kweon, Y. C., Kim, M. H. Cho, H. J., Kang, I. S. and Kim, S. J. (1996) Effects of an electric field on the nucleate pool boiling and bubble behavior on a horizontal wire. In *Convective Flow Boiling*, ed. J. C. Chen. Taylor & Francis, Bristol, pp. 351–356.

Lovenguth, R. F. (1968) Boiling heat transfer in the presence of electric fields. Ph.D. Thesis, Department of Chemical Engineering, Network College of Engineering, NJ.

Melcher, J. R. and Taylor, G. I. (1969) Electrohydrodynamics: A review of the role of interfacial shear stress. *Ann. Rev. Fluid Mech.* **1,** 111–146.

Miksis, M. J. (1981) Shape of a drop in an electric field. *Phys. Fluids* **24**(11), 1967–1972.

Ogata, J. and Yabe, A. (1991) Augmentation of nucleate boiling heat transfer by applying electric fields: EHD behavior of boiling bubble. *Proc. 3rd ASME/JSME Thermal Eng. Conf.*, Vol. 3, pp. 41–46.

Ogata, J. and Yabe, A. (1993) Basic study on the enhancement of nucleate boiling heat transfer by applying electric fields. *Int. J. Heat Mass Transfer* **36**(3), 775–782.

Ohadi, M. M., Papar, R. A., Ng, T. L., Faani, M. A. and Radermacher, R. (1992) EHD enhancement of shell-side boiling heat transfer coefficients of R-123/oil mixture. *ASHRAE Trans. Symp.* **BA-92-5-1,** pp. 427–434.

Pohl, H. A. (1958) Some effects on non-uniform fields on dielectrics. *J. Appl. Phys.* **29**(8), 1182–1188.

Purcell, E. M. (1965) *Electricity and Magnetism—Berkeley Physics Course*, Vol. 2. McGraw-Hill, London.

Stratton, J. A. (1941) *Electromagnetic Theory*. McGraw-Hill, New York.

Takuma, T., Kawamoto, T. and Sunaga, Y. (1985) Analysis of calibration arrangements for a.c. field strength meters. *IEEE Trans. Power App. Syst.*, **PAS-104(2),** pp. 489–495.

Yabe, A., Mori, Y. and Hijikata, K. (1995) Active heat transfer enhancement by utilizing electric fields. *Annual Review of Heat Transfer*, ed, Chang-Lin Tien, Vol. 7, chap. 4. Begell House, New York.